(15) A. McKillop, B. P. Swann, and E. C. Taylor, *J. Am. Chem. Soc.*, **93**, 4919 (1971).
(16) I. S. Dennis, J. K. M. Sanders, and J. C. Waterton, *J. Chem. Soc., Chem. Commun.*, 1049, (1976).
(17) E. Haslinger, *Monatsh. Chem.*, **109**, 523 (1978).
(18) H. Falk, E. Haslinger, and T. Schlederer, *Monatsh. Chem.*, in press.
(19) H. Falk, K. Grubmayr, E. Haslinger, T. Schlederer, and K. Thirring, *Monatsh. Chem.*, **109**, 1451 (1978).
(20) W. S. Sheldrick, *J. Chem. Soc., Perkin Trans. 2*, 1457 (1976).
(21) F. James and M. Roos, *Comput. Phys. Commun.*, **10**, 343–367 (1975).
(22) Equation 12 in ref 9 contains a computation error; all correlation times given there are too long. The correct expression is eq 7 in this paper.

# Quantitative Measurement of Intermediate Species in Sustained Belousov–Zhabotinsky Oscillations

**C. Vidal,* J. C. Roux, and A. Rossi**

*Contribution from the Centre de Recherche Paul Pascal, Domaine Universitaire, 33405 Talence Cédex, France.* *Received July 11, 1979*

**Abstract:** Sustained Belousov–Zhabotinsky oscillations have been performed in an open continuous-fed reactor, controlled by a computer. A procedure of repeated storage and accumulation of the signal given by any kind of detector allows the identification of several intermediate species and their concentration measurement with a good accuracy. By means of spectrophotometric as well as potentiometric techniques we have so obtained the concentration time dependence of $Ce^{3+}$, $Ce^{4+}$, $Br_2$, $Br^-$, bromomalonic compounds (BrMA), $O_2$, and $CO_2$. These species cannot account for the overall light absorption in the UV range (280–320 nm), so that at least another one, which we could not identify, is involved. A detailed analysis of our experimental results points out for a general agreement with the mechanism already proposed by Field, Körös, and Noyes.

Whereas the oscillatory behavior of the Belousov–Zhabotinsky (BZ) reaction has been studied under various conditions, the oscillating species yet identified experimentally in this system are few. Furthermore, very little is known about the phase differences in the temporal oscillations of these species. Nevertheless, Field, Körös, and Noyes (FKN) proposed some years ago[1] a kinetic model accounting for the temporal and spatial patterns of the BZ reaction. Even if this mechanism appears to be rather successful and its basic assumptions probably valid, no general examination has ever been carried out, owing to the lack of reliable and detailed experimental results. The aim of our work is just such an examination, which in the first place presupposes the collection of a wide set of experimental data.

## I. Experimental Section

**1. Apparatus.** An experimental device, allowing the study of any oscillating reaction in such a way that quantitative and reliable information should become available, has been developed in our laboratory. Since full details appear in previous papers,[2] let us recall only briefly its basic features.

In a continuous-flow stirred tank reactor, fed with reagent solutions at a constant rate, the chemical oscillations can be made highly reproducible. Figure 1 shows, for instance, the high stability of the period reached in a typical experiment on the BZ reaction. Our apparatus, designed to take advantage of this fact, can thus increase as desired the signal to noise ratio of any signal originating in the chemical oscillating system. In short, after each oscillation, the signal given by the detector (spectrophotometer, ion-specific electrode, thermocouple, etc.) is stored and accumulated on a minicomputer (Digital LSI 11). The storage and accumulation procedure is stopped when the accumulated signal is no longer noisy, which is checked on a video terminal. Then the data are transferred to another computer (Digital VAX 11/780) and recorded on its mass memory, so that they are available for subsequent numerical analysis. Each record, 500 points long, covers one and a quarter period.

**2. Experiments.** Two different experiments have been carried out on the BZ reaction with this device. The main difference between them lies in the catalyst chosen, $Ce^{3+}$ in the first case and $Mn^{2+}$ in the second, for reasons which will become clear later. The reactor volume is 28 $cm^3$ and mixing is ensured by a glass stirrer rotating at a constant speed of 600 rpm. Other experimental constraints are as given in Table I.

All figures in this paper, excepting Figures 6 and 7, refer to the cerium experiment.

**3. Results.** When the detector in use is a spectrophotometer (Cary 16), the optical density of the reacting medium can be stored at several wavelengths by repeating the procedure described in section II. These different temporal oscillations put together form a matrix, the representation of which is given in Figure 2. We did not try to record the optical density beyond 570 nm because the amplitude of its variation—as well as its absolute value—is too low. On the other hand, below 280 nm the optical density becomes too high (>2) and is no longer measurable. It is quite obvious in Figure 2 that crossing between the stored temporal oscillations and a plane perpendicular to the time axis provides the absorption spectrum of the reacting medium at any given time. An example is displayed in Figure 3, where circles stand for the measured optical density.

In principle the analysis of such a spectrum allows one to determine which species are responsible for the light absorption and to compute the corresponding concentrations. Nevertheless one has to make some assumptions before any calculation can be done. We have divided the field of wavelengths into two parts, assuming that above 320 nm only $Ce^{3+}$, $Ce^{4+}$, $Br_2$, HBrO, $HBrO_2$, and $BrO_2$ radical[3] are—or might be—encountered. The overall concentration of cerium ions is, of course, time independent, its absolute value being equal to the $Ce^{3+}$ inlet concentration. On a first glance at Figure 3, one sees that $Ce^{4+}$ is the main absorbing species in this "*visible*" region. It is unlikely that $HBrO_2$ or HBrO could be detected when cerium is used as a catalyst: a high concentration of these species would be necessary, because of the great difference between their molar extinction coefficient and the $Ce^{4+}$ one. However, cerium ions cannot account by themselves for the overall optical density and at least another species is required. In a first step we tried to fit our results with the set $Ce^{3+} + Ce^{4+}$ and $BrO_2$·, since the discovery of this radical in the BZ reaction has been recently reported.[4] Unfortunately this attempt failed, least-squares fitting even leading sometimes to negative values of the $BrO_2$· concentration. On the contrary, when the set $Ce^{3+} + Ce^{4+}$, $Br_2$ is taken, the fit looks much better. It can still be improved if three independent components are used: $Ce^{3+} + Ce^{4+}$, $Br_2$, $BrO_2$·. However, the same is also achieved with the set $Ce^{3+} + Ce^{4+}$, $Br_2$, continuous absorption at a low level (never more than 0.03 in optical density). In other words, the improvement is insensitive to the shape of the third component spectrum. Hence our results indicate that bromine is an intermediate species in the BZ reaction, whereas they do not allow one to draw any conclusion about the $BrO_2$· radical.

What happens, now, in the UV region, i.e., between 280 and 320 nm? The contribution of $Ce^{3+}$, $Ce^{4+}$, and $Br_2$ to the optical density is easily computed, since the concentrations of these three species are provided by the previous fit. The experimental light absorption being higher, some other species have to be taken into account. In the range of wavelengths under examination bromate and malonic acid are not

0002-7863/80/1502-1241$01.00/0 

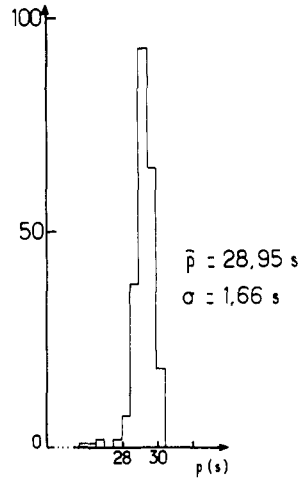


**Figure 1.** Typical period distribution histogram.

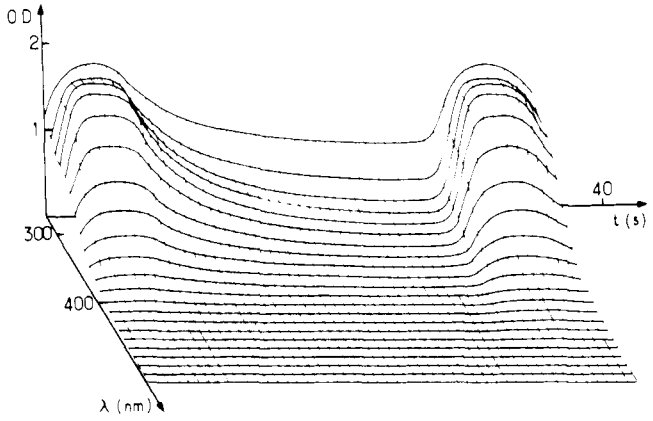


**Figure 2.** Temporal oscillations of the optical density at different wavelengths.

**Table I**

| | Ce expt | Mn expt |
|---|---|---|
| mean temp $T$, °C | 40 | 54.5 |
| mean residence time $\tau$, s | 1680 | 480 |
| concn of inlet species after mixing and before any reaction, mol $L^{-1}$ | $CH_2(COOH)_2$: 0.08<br>$KBrO_3$: 0.036<br>$H_2SO_4$: 1.5<br>$Ce_2(SO_4)_3$: 0.000 25 | $CH_2(COOH)_2$: 0.017<br>$KBrO_3$: 0.023<br>$H_2SO_4$: 1.5<br>$MnSO_4$: 0.0012 |

significantly absorbent. One's first guess would be that bromomalonate (BrMA) is involved and we have therefore measured the absorption spectrum of this species.[5] The shape of this spectrum is quite different from the remaining optical density, once absorption by $Ce^{3+}$, $Ce^{4+}$, and $Br_2$ has been subtracted: a fifth species is required at least. We could not identify this "*unknown*" species, named X, although its absorption spectrum obtained by trial and error seems to look like the curve of Figure 6. Assuming the presence of X and BrMA, a least-squares fit between 280 and 320 nm gives us the concentration of these two species. Figure 3 shows as an example the correlation between the experimental (circles) and computed (full line) optical densities, together with the contribution of the five species (dotted lines). The same numerical analysis of the absorption spectrum, repeated at each oscillation, provides the time variations of these concentrations displayed on Figure 4. The following are also plotted: (1) the redox potential measured between a Pt and a $Hg/Hg_2SO_4$ reference electrode; (2) the bromide concentration determined by a bromide-ion specific electrode (Philips IS 550); (3) the concentration of dissolved oxygen given by an $O_2$ polarographic cathode (Radiometer E 5140) after correction for its response time.

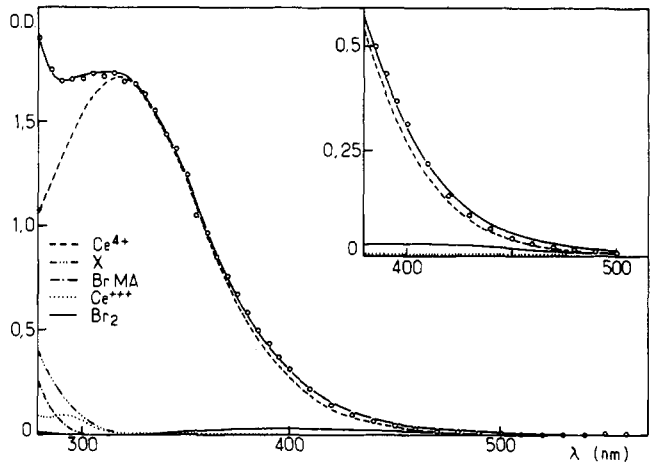


**Figure 3.** Absorption spectrum computed (full line) from the five involved species, compared with experimental values (circles) at time $t$ = 5.1 s.

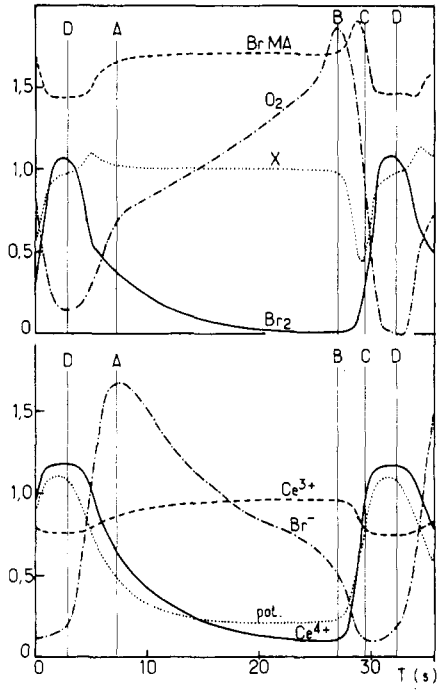


**Figure 4.** Temporal (about one and a quarter period) oscillations in concentration of measured species. One vertical unit represents (mol $L^{-1}$): BrMA, $5 \times 10^{-3}$; $Br_2$, $1 \times 10^{-4}$; $Br^-$, $2.5 \times 10^{-4}$; $Ce^{3+}$, $5 \times 10^{-4}$; $Ce^{4+}$, $1 \times 10^{-4}$. $O_2$, X, and redox potential arbitrary.

Using a $CO_2$ cathode (Radiometer E 5037-0) it can be easily ascertained that there is no oscillation in the concentration of dissolved carbon dioxide, the solution always being saturated.

We have shown elsewhere[2c,6b] how the chemical reaction contribution to the concentration changes inside the reactor can be obtained by a very simple calculation. One has to take into account the flux through the reactor on one hand, and to compute the first derivative of the concentration vs. time curves on the other; then the overall chemical reaction rate for each species is merely given by the related balance equation. Such a derivation applied to the curves of Figure 4, followed by a correction for the flux term, leads to the result displayed in Figure 5. Each reaction rate can be either positive or negative depending upon which prevails between production and consumption steps of the involved species. Let us emphasize that these curves plotted on Figure 5 are now a salient feature of the chemical reaction itself.

In the second experiment (Mn expt) we took $Mn^{2+}$ as the catalyst in order (1) to confirm the occurrence of the unknown species X and (2) to set up a new attempt at identifying and measuring possible absorption due to $HBrO_2$ and/or HBrO. Manganese is very suitable for this last purpose because it does not yield any species with high

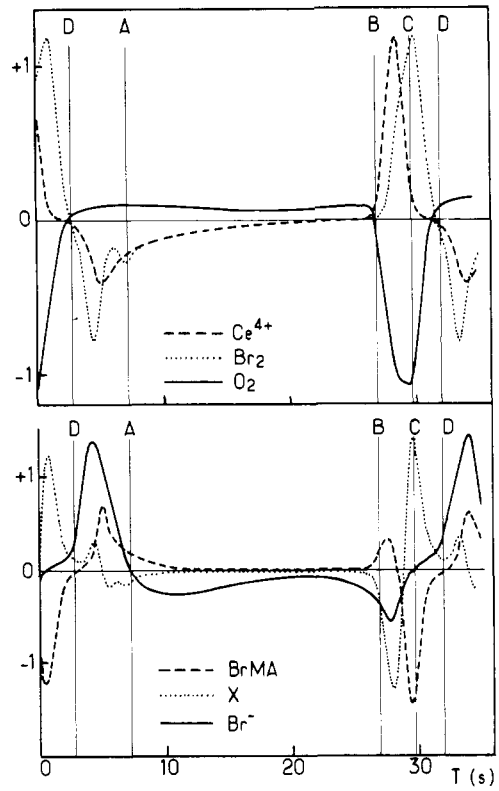


**Figure 5.** Overall chemical reaction rates.[12] One vertical unit represents (mol $L^{-1}$ $s^{-1}$): BrMA, $1 \times 10^{-3}$; $Br^-$, $1 \times 10^{-4}$; $Br_2$, $5 \times 10^{-5}$; $Ce^{4+}$, $5 \times 10^{-5}$. $O_2$ and X arbitrary.

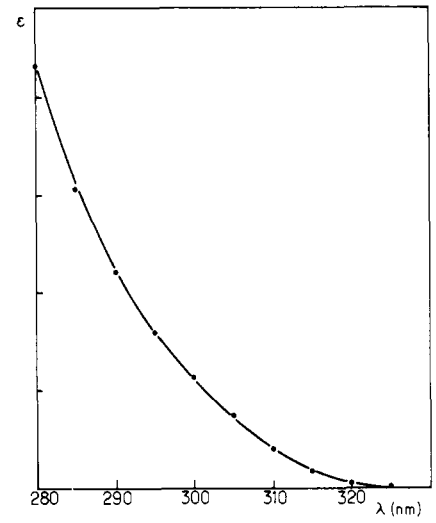


**Figure 6.** Assumec absorption spectrum of the unknown species X.

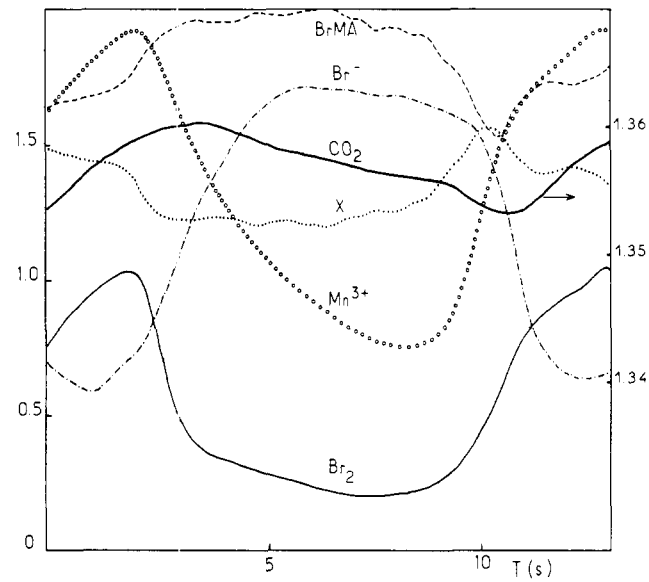


**Figure 7.** Temporal (about one and a quarter period) oscillations in concentration of measured species during the $Mn^{2+}$-catalyzed reaction. One vertical unit represents (mol $L^{-1}$): BrMA, $5 \times 10^{-3}$; $Br_2$, $2 \times 10^{-5}$; $Br^-$, $2 \times 10^{-4}$; $Mn^{3+}$, $5 \times 10^{-5}$; X, arbitrary. $CO_2$: right scale in $10^{-2}$ mol $L^{-1}$.

extinction coefficient in the range 300–350 nm. The analysis of experimental spectra between 280 and 700 nm in a manner closely related to the one previously described points to the fact that four species are involved: $Mn^{3+}$, $Br_2$, BrMA, and unknown X (same spectrum as before). Moreover, in this case too, $HBrO_2$ and HBrO as well as $BrO_2\cdot$ do not bring any measurable contribution to the light absorption. If we take an optical density of 0.05 as the upper limit to escape notice, it follows from all our results that the concentrations of these three species never exceed $1 \times 10^{-4}$ ($HBrO_2$), $6 \times 10^{-5}$ (HBrO), and $2 \times 10^{-5}$ mol $L^{-1}$ ($BrO_2\cdot$).

The temporal oscillations in $Mn^{3+}$, $Br_2$, BrMA, and X concentrations are plotted in Figure 7 together with those of $Br^-$ and $CO_2$ determined in the same way as above. No oscillation in dissolved oxygen could be detected, because its concentration always remains very close to zero.

Up to this point the conclusions which can be drawn from these two experiments are (1) some evidence for an unknown species X absorbing in the UV region (Figure 6); (2) an upper limit of $HBrO_2$, HBrO, and $BrO_2\cdot$ concentration lying between $2 \times 10^{-5}$ and $10^{-4}$ M.

## II. Interpretation

In 1972 Field, Körös, and Noyes[1] proposed a mechanism—and later on the "*Oregonator*" model—taking into account the experimental observations available at that time, i.e., the oscillations in $Br^-$ and $Ce^{4+}$ concentrations. However, these oscillations, performed in closed reactors, were not sustained and the accuracy of the measurements was not very high. Our work brings a lot of quantitative experimental facts and thus allows us to check the grounds of the FKN mechanism on a wide basis.

For this purpose we will discuss mainly Figures 4 and 5, where five vertical lines (D, A, B, C, D) have been plotted dividing the temporal oscillation into four parts. As a matter of fact we must try to identify the essential features of the four steps distinguished by FKN. Lastly the labeling of chemical reactions will be the same as in the original FKN paper.

**Step 1.** When the bromide concentration is high enough, bromate is reduced by a two-electron process:

$$2H^+ + BrO_3^- + Br^- \rightarrow HBrO_2 + HBrO \qquad (R3)$$

$$H^+ + HBrO_2 + Br^- \rightarrow 2HBrO \qquad (R2)$$

During this step $Br^-$ is slowly consumed as in the AB part of the oscillation.

**Step 2.** If the bromide concentration becomes too low (line B), reaction R2 no longer competes with reaction R5, and the system switches to a one-electron process:

$$H^+ + BrO_3^- + HBrO_2 \rightarrow 2BrO_2\cdot + H_2O \qquad (R5)$$

followed by

$$BrO_2\cdot + Ce^{3+} + H^+ \rightarrow HBrO_2 + Ce^{4+} \qquad (R6)$$

The concentration of $HBrO_2$ grows autocatalytically, increasing the rate of $Br^-$ consumption by the reaction R2; hence, the bromide concentration drops with increased speed, while the $Ce^{4+}$ concentration rises. This is closely observed in the BC range of the curves.

**Step 3.** The $Ce^{4+}$ ions produced by (R6) react with bromi-

nated organic species:

$$4Ce^{4+} + BrCH(COOH)_2 + 2H_2O \rightarrow 4Ce^{3+} + Br^- + HCOOH + 2CO_2 + 5H^+ \quad (R10)$$

Bromide is released and its concentration begins to increase, but rather slowly because the autocatalytic process remains active. This happens between lines C and D.

**Step 4.** When the autocatalysis vanishes, bromide ions are only consumed in the slow process (R2-R3) and still produced by (R10). Therefore their overall rate of production increases, while the concentration of $Ce^{4+}$ falls since the source (R6) is now switched off. This step takes place between D and A, until the rate of (R10) slows down so that a new cycle may begin.

It is not really surprising to find a good agreement between the FKN mechanism and our results on temporal oscillations of $Br^-$ and $Ce^{4+}$ concentrations. Of course it will be more interesting to see how this model is able to account for the other species measured.

According to the FKN mechanism bromomalonic acid (BrMA) is produced in two ways, either

$$H^+ + Br^- + HBrO \rightarrow Br_2 + H_2O \quad (R1)$$

$$Br_2 + CH_2(COOH)_2 \rightarrow BrCH(COOH)_2 + H^+ + Br^- \quad (R8)$$

or

$$CH_2(COOH)_2 + HBrO \rightarrow BrCH(COOH)_2 + H_2O \quad (R'1)$$

In fact this last reaction has been suggested because the occurrence of bromine as an intermediate species was not clearly established.[4,7] However, Geiseler[11] has shown that, between 440 and 540 nm, $Ce^{4+}$ ions alone cannot account for the overall light absorption. He tentatively attributed the remaining absorption to bromine. The sink term of BrMA is reaction R10, which implies first the radical oxidation[8,9] of malonic acid:

$$Ce^{4+} + CH_2(COOH)_2 \rightarrow \dot{C}H(COOH)_2 + Ce^{3+} + H^+ \quad (RR1)$$

followed by

$$\dot{C}H(COOH)_2 + BrCH(COOH)_2 \rightarrow Br\dot{C}(COOH)_2 + CH_2(COOH)_2 \quad (RR2)$$

and by

$$Br\dot{C}(COOH)_2 + H_2O \rightarrow Br^- + H^+ + \dot{C}OH(COOH)_2 \quad (RR3)$$

Our results are in qualitative agreement with this assumption. In the AB part of the oscillation the sink and source terms balance each other: there is little or no production of BrMA. Beyond line B the increase in the rate of (R2) is assumed to induce a parallel growth in the rate of (R1) and/or (R'1). This may explain the small rise observed in the BrMA concentration. But soon the $Ce^{4+}$ concentration reaches a level where the reaction RR1 prevails, involving the observed fall in [BrMA]. There is no longer a rapid decrease in $[Br^-]$ but rather a slow increase (reaction RR3), the autocatalytic consumption of $Br^-$ ions being still active, as already outlined.

Does the autocatalytic process stop at time D as predicted by the FKN mechanism? Once more, our results seem to be in favor of such a statement. As a matter of fact the rapid increase in $[Br^-]$ beyond line C may originate either from cancellation of the sink term or from an increase in the source one. Now, $[Ce^{4+}]$ and [BrMA] remaining roughly constant, no drastic change is to be expected in the source term of $Br^-$ ions, closely related to the rate of reaction R10. Therefore we must conclude that there is a lowering in the rate of bromide-consuming reactions. This will indeed be the case if $[HBrO_2]$ is also decreasing, so that the autocatalytic production of this species will finally stop. Later on, when $[Ce^{4+}]$ begins to decrease, the reaction RR1 slows down and so does the overall reaction R10, allowing [BrMA] to rise.

The autocatalytic process switches on and off for two different values of $[Br^-]$ (see Figure 4: $[Br^-]_B > [Br^-]_D$). This result was first pointed out by Field, Körös, and Noyes,[1a] who, in their original paper, attributed it to the higher $Ce^{4+}$ concentration at point D than at point B.

In a recent paper[9] we confirmed the occurrence of sequence (RR1-RR3), giving some experimental evidence that the $Ce^{4+}$ oxidation of malonic acid is followed by an oxygen consumption, according to

$$O_2 + \dot{C}H(COOH)_2 \rightarrow \dot{O}OHC(COOH)_2$$

The direct proof is shown in Figures 4 and 5, where oxygen appears to be consumed when the reactions RR1-RR3 take place, i.e., during the BCD phase of the oscillation. Furthermore, our results show unambiguously that part of the visible absorption is due to bromine.

The bromine concentration remains, of course, very low, even at its maximum, which indicates that the (R8) reaction is much faster than its equivalent in iodine chemistry.[9] We must also point out that our finding of $Br_2$ as an intermediate species supports the recent work of Edelson, Noyes, and Field,[10] who, modifying slightly the FKN mechanism, assume the rate of reaction R'1 to be zero. The observed increase in bromine concentration during the autocatalytic process (B-D) may be explained if the rate-determining step of sequence (R1-R8) is (R8), which implies a "*high*" enough concentration of HBrO. And precisely, this condition can only be fulfilled when the autocatalytic production of $HBrO_2$ induces a sudden rise in [HBrO].

We have already mentioned that the medium always remains saturated by $CO_2$ during the course of the cerium-catalyzed reaction. This means that the rate of carbon dioxide producing reactions is high enough to keep the solution saturated at atmospheric pressure, while physical release to the atmosphere is fast enough to prevent supersaturation. On the contrary, $[CO_2]$ appears to be time dependent in the manganese-catalyzed experiment. Figure 7 shows that temporal oscillations in $CO_2$ and BrMA concentrations are closely related; in other words, no time lag is observed between the production of BrMA and of $CO_2$. Accordingly the lifetime of intermediate species leading from BrMA to $CO_2$ is short, a result which is in agreement with recent computational work.[10] Since the unknown species X and BrMA oscillate in opposite phase, the first cannot belong to this set of intermediate species. Let us add, lastly, that the absorption spectrum of bromoacetic acid, a well-known degradation product of malonic acid, has nothing to do with those of X. Hence the identity of X would still seem to remain unknown.

In conclusion, one has to state that there is a full qualitative agreement between the main features of the BZ reaction predicted by the FKN mechanism and our own experimental observations. However, two important questions remain to be answered. (i) What chemical species oscillates in opposite phase with BrMA as the unknown X does? (ii) How far can the Field, Körös, and Noyes mechanism account for these experimental results in a quantitative manner?

**Acknowledgment.** The authors are indebted to S. Sanchez and G. Gabriel for technical assistance in computer handling and to one referee for bringing to their attention Geiseler's work.

## References and Notes

(1) (a) Field, R. J.; Körös, E.; Noyes, R. M. *J. Am. Chem. Soc.* **1972**, *94*, 8649. (b) Field, R. J.; Noyes, R. M. *J. Chem. Phys.* **1972**, *60*, 1877. (c) Edelson, D.; Field, R. J.; Noyes, R. M. *Int. J. Chem. Kinet.* **1975**, *7*, 417.

(2) (a) Roux, J. C.; Sanchez, S.; Vidal, C. *C. R. Acad. Sci. Ser. B* **1976**, *282*, 451. (b) Roux, J. C.; Vidal, C. *C. R. Acad. Sci., Ser. C* **1977**, *284*, 293. (c) Vidal, C.; Roux, J. C.; Rossi, A. *Ibid.* **1977**, *284*, 585.
(3) The absorption spectrum of $BrO_2^-$ in the range 300–600 nm is given by Buxton, G. V.; Dainton, F. S. *Proc. R. Soc. London, Ser. A* **1968**, *304*, 427.
(4) Forsteling, H. D.; Schreiber, H.; Zittlau, W. *Z. Naturforsch. A* **1978**, *33*, 1552.
(5) In fact only a mixture of monobromo- and dibromomalonic acid has been prepared since these two species cannot be separated. See, for instance, Bornmann, L.; Busse, H.; Hess, B. *Z. Naturforsch. B* **1973**, *28*, 93. Therefore BrMA stands for the mixture.
(6) (a) Roux, J. C.; Vidal, C. "Synergetics", Vol. 3, "Far from Equilibrium"; Springer-Verlag: West Berlin, 1979; p 47. (b) *Nouveau J. Chim.* **1979**, *3*, 247.
(7) Zhabotinsky, A. M. *Biophysics* **1964**, *9*, 329.
(8) Jwo, J. J.; Noyes, R. M. *J. Am. Chem. Soc.* **1975**, *97*, 5422.
(9) Roux, J. C.; Rossi, A. *C. R. Acad. Sci., Ser. C* **1978**, *287*, 151.
(10) Edelson, D.; Noyes, R. M.; Field, R. J. *Int. J. Chem. Kinet.* **1979**, *11*, 155.
(11) (a) Geiseler, W. Thesis, RWTH Aachen, West Germany, 1974. (b) Franck, U.; Geiseler, W. *Naturwissenschaften* **1970**, *58*, 52.
(12) Thanks to the very low absolute value of $[O_2]$ (<0.5 Torr) the weak oxygen production during the DB part of the oscillation might be meaningless.

# Correlations of Gas-Phase Acidities and Basicities with the Electrostatic Field Model

**Carolyn S. Yoder and Claude H. Yoder***

*Contribution from the Department of Chemistry, Franklin and Marshall College, Lancaster, Pennsylvania 17604.* *Received March 12, 1979*

**Abstract:** The potential energies of charge–dipole, charge-induced dipole, and dipole–dipole interactions in sets of substituted acetic acids, benzoic acids, phenols, and pyridines were calculated from the classical equations for these interactions and then correlated with the enthalpy changes for the gas-phase dissociations (or proton affinities) of these compounds. The correlation coefficients for the least-squares fit of $\Delta H°$ with the charge–dipole potential energy in the conjugate base (acid) were greater than 0.95 for most of the series. Moreover, the relative magnitudes of the potential energies agreed well with the relative magnitudes of the enthalpy changes. Addition of the charge-induced dipole energy to the charge–dipole energy improved the correlations in sets with low-polarity, polarizable substituents. Hence, the electrostatic field effect can be used to quantitatively correlate the effect of substituents on gas-phase acidities and basicities. Moreover, for systems containing polar substituents, the predominant field effect, indeed probably the predominant substituent effect, is the charge–dipole interaction in the conjugate ion.

The relative gas-phase acidity and basicity data collected over the past decade have been analyzed or correlated with the polarizability (charge-induced dipole field) effect,[1a] molecular orbital theory,[1b] the proton potential model,[1c] the electrostatic potential surrounding a base,[1d] core-ionization energies,[1e] and a variety of other molecular and atomic parameters such as electronegativity, hybridization, bond energies, and electron affinities.[1f] Although the charge-induced dipole field effect is widely invoked, especially in qualitative explanations of the relative acidities or basicities of alkyl homologues,[1a,2] only a few attempts have been made to employ simple classical electrostatic interactions in quantitative correlations. Aue, Webb, and Bowers showed that the charge-induced dipole interaction could account for the difference in proton affinities in a series of four primary alkylamines,[3] while Kollman and Kenyon used the charge–charge interaction to successfully predict the second proton affinities of a series of diamines.[4]

We present here an attempt to evaluate the electrostatic field effects of substituents on the gas-phase dissociation (1) and protonation (2) reaction:

$$X\text{-}A\text{-}H \rightarrow X\text{-}A^- + H^+ \quad (1)$$

$$X\text{-}B + H^+ \rightarrow X\text{-}B\text{-}H^+ \quad (2)$$

The most important electrostatic interactions between the substituents and the reaction site are the charge–dipole and charge-induced dipole interactions in the conjugate ions of (1) and (2) and the dipole–dipole interaction in the free acid of (1) and the base of (2). These field effects will be most likely to control the relative extents of (1) and (2) when (a) the substituent effects on the A–H and B–H bond energies are minor; that is, when the A or B moieties of a given series of acids or bases moderate the influence of X on the A–H or B–H bond energies; (b) inductive, resonance, and steric substituent effects are small or parallel the field effects; (c) substituent-induced changes in $\Delta S°$ are small.

For the series of compounds studied here the substituent-induced changes in $\Delta S°$ are likely to be negligible[5,6] and therefore the correlation of these field effects with the experimentally determined enthalpies of dissociation and proton affinities should permit an evaluation of the hypothesis that field effects control (in the predictive sense) the relative acidities or basicities within a given series. These correlations should also provide information on the relative importance of the charge–dipole, charge-induced dipole, and dipole–dipole interactions.

The four systems studied include a set (I) of 9 substituted acetic acids, a set (II) of 19 substituted benzoic acids, a set (III) of 13 phenols, and a set (IV) of 10 substituted pyridines. For the acids, the charge–dipole and charge-induced dipole potential energies were calculated for the interaction of the substituents with the negative charge of the conjugate ion, and the dipole–dipole energy was calculated for the interaction of the substituent with the reaction site (COOH for sets I and II, OH for III). For the pyridines, the charge–dipole and charge-induced dipole energies were determined for the substituted pyridinium ion and the interaction of the substituents with the dipole due to the heteroatom was calculated for the substituted base.

The calculations of these field effects were performed with the classical equations for these effects:

$$V_c = \frac{-q\mu \cos\theta}{\epsilon r^2} \qquad \text{charge–dipole}$$

$$V_I = \frac{-q^2\alpha}{2\epsilon r^4} \qquad \text{charge-induced dipole}$$

$$V_D = \frac{-\mu_1\mu_2(2\cos\theta\cos\phi - \sin\theta\sin\phi)}{\epsilon r^3} \qquad \text{dipole–dipole}$$

0002-7863/80/1502-1245$01.00/0 